Experimental study on the vertical deformation of sand caused by cyclic withdrawal and recharging of groundwater

Yuqi Li[a], Zaile Hu[a], Tianquan Weng[a], Joana Fonseca[b], Xiaodi Zhang[a]

[a] Department of Civil Engineering, Shanghai University, Shanghai 200072, China

[b] Department of Civil Engineering, City University London, London EC1V 0HB, UK

ABSTRACT: Fast urban growth and an ever-increasing frequency of extreme weather-related events demand a better understanding of land subsidence and the potential measures to control it. This paper presents an experimental investigation on the deformation behaviour of sand undergoing cyclic withdrawal and recharging of groundwater. A sand-box model with dimensions 1000 mm × 600 mm × 892 mm was used to investigate soil deformation following lowering and rising of the water table. The sand used was Pingtan sand (Fujian, China) a quartzitic formation composed of elongated to slightly spherical grains. Three sand samples with different initial densities, i.e. loose, medium dense and dense, were tested on repeated cycles. The vertical deformation of the sand was measured and the corresponding strain and effective stress were calculated. The observations show that initially the sand behaves as an elastic material with the subsidence caused by water withdrawal being recovered as the soil rebounds during recharging. With further withdrawal-recharging cycles, subsidence becomes larger as plastic deformations as well as time-dependent deformation occur in the soil. The distinct patterns of deformation were identified to be dependent on both the initial density and the number of withdrawal- recharging cycle the sand has been subjected to. The different behaviour of the medium dense sample compared to the loose and dense samples, in particular for the first two cycles, indicates that the soil response cannot be explained in respect of the initial void ratio alone and further microstructure considerations were discussed. It is suggested that the orientation of the grains resulting from the sample preparation technique and the consequent induced anisotropy can be used to explain the results herein presented. Finally this paper provides the rationale for a micromechanical interpretation of soil deformation when subjected to changes in stress due to rising or lowering of the water table, which will help in establishing measures to control land subsidence, in particular to assess the efficiency of water recharging following subsidence by withdrawal.

KEYWORDS: subsidence; resilience; withdrawing water test; recharging water test

1 INTRODUCTION

Since the late 19th century, the intensification of human activities has led to a series of man-made disturbances with the potential to cause ground-engineering problems, land subsidence is an example. Land subsidence is the lowering or collapsing of the ground surface caused by natural phenomena as heavy rain or anthropogenic activities including the exploitation of groundwater, oil or gas resources or any other changes in drainage pattern caused by the excavation of the underground. A significant number of cities and regions around the world have experienced subsidence to a certain extent (Zheng et al., 2005). Early cases of land subsidence were observed in Venice (Italy) and Mexico (Marsal and Sáinz, 1956) and subsequent observations were reported in various other cities and countries across the world, e.g. in Japan (Sato et al., 2003), China (Shi and

Bao, 1984), USA (Allen and Mayuga, 1969), Europe (Teatini et al., 2005) and Southeast Asia (Phien-wej et al., 2006). Furthermore, Ortiz and Ortega (2010) have reported subsidence values as high as over 13 m, a value measured in 2006 in the Chalco Plain near Mexico City. In China, in particular, land subsidence has been mainly reported in the Yangtze River delta, the North China plain and the Fen-Wei basin as a consequence of the groundwater or underground space exploitation in these areas (Ministry of land and resources of the People's Republic of China and Ministry of water resources of the People's Republic of China, 2012).

Land subsidence causes flooding in rural low-lying areas and sea water invasion in coastal cities, which has a direct effect on the agricultural production, disrupts activities of the port facilities and also causes uneven subsidence of foundations and damage of buildings and other infrastructures (Pan and Li, 2012). For all the above reasons, ground vertical deformation (subsidence and rebound) has become a topic of interest in the field of geotechnical engineering practice and research. Previous studies have investigated the relationship between deformation and the change of groundwater level based on the deformation characteristics of the soil layers from observation data of ground subsidence and water level (Ye et al., 2005; Zhang et al., 2006, 2012; Shi et al., 2008; Wang et al., 2009; Wu et al., 2010; Miao et al., 2011; Lv et al., 2011). In addition, various models were used to simulate land subsidence caused by groundwater pumping, e.g. viscous-elastic-plastic models, consolidation-seepage-creep coupling models and flow and subsidence coupling models. For example, based on Biot's consolidation theory, Luo and Zeng (2011) established a viscoelastic plasticity finite element model with seepage and soil skeleton deformation coupling, and simulated ground subsidence caused by underground water exploitation in Cangzhou, China. The recent developments in imaging and radar technology have allowed the use of Interferometric Synthetic Aperture Radar technology to study land subsidence. Examples of application of this technology include Orihuela city in Spain (Tomas et al., 2010), Yunlin County of central Taiwan (Tung & Hu, 2012) and the central region of Mexico (Chaussard et al., 2014). Scanning electron microscopy images of the pore structure of soil before and after centrifuge model tests of groups of high-rise buildings were used for the study of land subsidence and the change of the macrostructure and microstructure characteristics of soil (Cui and Jia, 2013). Aviles and Pérez-Rocha (2010) presented an empirical method to evaluate the effects of regional subsidence caused by groundwater extraction during seismic events in Mexico City. Land subsidence due to groundwater extraction can give rise to secondary disasters such as earth fissure and ground failure, as reported in previous studies (Budhu, 2011; Pacheco-Martínez et al., 2013).

The viscous behaviour of clay has been a subject of numerous studies (Kutter and Sathialingam, 1992; Fodil et al., 1997; Yin and Zhu, 1999; Yin et al., 2002; Karim et al., 2010). While the viscous behaviour of sand has been overlooked mainly because it is usually regarded as a non-viscous material. A few significant studies on the creep behaviour of sand related to land subsidence of sand strata are referenced herein. Lade et al. (1997) have carried out a series of experiments to investigate the effect of strain rate and creep on the onset of instability, the yield surface movement under drained conditions and the pore water pressure development under undrained conditions. An elastic viscoplastic model for sand to account for time-dependent behaviour and strain rate effects has been proposed by Boukpeti et al. (2004). Zhang et al. (2006) analyzed the influence of the lowering and rising of the water table in the sand deformation and identified three distinct modes of behaviour: elastic behaviour in the periods of groundwater table ascending or being steady, elasto-plastic behaviour when the groundwater table was higher than the lowest recorded value and visco-elasto-plastic behaviour when the groundwater table was lower than the lowest recorded value.

Large parts of the studies mentioned above rely on observation data in order to establish land subsidence models by analyzing the deformation characteristics of soil and land subsidence behaviour. Land subsidence surveys can, however, be extremely costly both in terms of time and money required, hence a laboratory-scale model test presents a more convenient method to study soil subsidence due to groundwater extraction. In the present study, a laboratory test model was designed, and sand subsidence and rebound by cyclic withdrawing and recharging of water was investigated. Three samples of sand with different densities, i.e. loose, medium dense and dense were tested. The vertical deformation was recorded during the repeated lowering and rising of the water table and the effective stress and strain were calculated for these different stages.

2 EXPERIMENTAL SET-UP AND MATERIAL

2.1 *Laboratory model*

The experimental device comprises a model box connected to a series of pipes and the measurement equipment. The size of the box was 1000 mm × 600 mm × 892 mm (length × width × height). The front and back sides of the box were made of glass to enable observations of the experimental phenomena and measurement of the vertical deformation of the soil. The lateral and bottom sides were made of steel plates. The lateral and front views of model box and the pipes are shown in Figure 1. In the inlet and outlet of the box, an 80 mm thickness cobble buffer layer was set in order to prevent soil disturbance caused by the flux of water. The inlet pipe (number 10 in Fig 1) was connected to the water pump and water reservoir. Drainage was allowed by opening valves 1 to 5 and 8 and closing valves 6 and 7. For the water recharge, valves 1 to 4, 6 and 7 were opened and valves 5 and 8 were closed.

2.2 *Sand description and sample preparation*

The sand used in the experiment was the standard Pingtan sand from Fujian, China. Pingtan sand is a natural quartzitic sand (approximately 96% SiO_2). Particle size distribution and the correspondent characteristic parameters, i.e. d_{50}, C_u and C_c, are shown in Tables 1 and 2, respectively. The range size of particles in this sand is relatively narrow, with most of the grains sized between 0.250 mm and 0.650 mm. The physical indexes of the sand are shown in Table 3. The grain morphology comprises a mixture of elongated grains and more spherical grains, rounded to sub-rounded. Three sand specimens with different densities and termed as loose sand, medium dense sand and dense sand hereafter, were obtained using the sample preparation techniques described in Table 4. The loose sand sample was obtained by dry pluviation with the sand poured from a very small distance to the sample surface. For the medium and dense sand, dry pluviation with a height drop of 400 mm was used. In addition, in the case of the dense sand, the soil was tamped with a hammer of 2.5 kg weight at the sample heights of 250 mm, 500 mm and 700 mm, respectively. The final densities attained are presented in Table 4. Given the different sample preparation techniques used, a different microstructure for each of the three samples is also expected in addition to the different initial densities, this will be discussed later in the paper. Given the large volume of sand required for each experiment, the same sand was used for the three tests and at the end of each experiment the dumped sand was dried in the sun and re-used.

2.3 *Experimental procedure*

(a) Saturation process

Following the sample preparation as described above, with a total height of 700 mm, the sample was left for 12 h in order for the internal forces within the sand to come into balance. The water was pumped into the box slowly to allow entrapped air to be eliminated. After the soil was immersed in the water, it was left for 24 h in order to saturate completely.

(b) Withdrawing test

In the withdrawing process, the lowering of the soil surface and water level was measured using a ruler fixed to the glass panel. The accuracy in the readings was guaranteed by acquiring digital images with a camera positioned in a perfect perpendicular plane to the ground surface and take the reading from the images was taken. When the water level dropped to approximately 200 mm, the withdrawing was stopped and the sample was left for 24 h (including withdrawal time) so that the water level and subsidence of sample gradually became stable.

(c) Recharging test

After the sample subsidence became stable, water was slowly recharged by controlling the inlet and outlet valves of the soil box (shown in Figure 1). When the water level was slightly above the soil surface, the recharging was stopped and the sample was left for 24 h (including recharging time) to stabilize the water level and subsidence of the soil. The withdrawing and recharging experiments were carried out for a number of times by successively repeating steps (b) and (c).

For both the withdrawing and recharging tests, the pre-set rate value of 250 mm/h (i.e. 500 mm/2 h) was occasionally affected by poor drainage due to sand plugging. This phenomenon has slowed down the processes of lowering the water table to 200 mm height after withdrawing and the rising of the water table to 700 mm height, following recharging. Another experimental drawback relates to the slight uneven ground surface following the change in the water table. The errors associated to these drawbacks are believed to be minor.

3 WATER LEVEL CHANGE AND VERTICAL DEFORMATION OF THE SOIL

Figures 2 to 4 show the variation of water table and vertical deformation under the conditions of cyclic withdrawing and recharging for the loose sand, medium dense sand and dense sand, respectively. For each cycle the water level is represented by the vertical bars for the withdrawing and recharging (taking the bottom of the box/soil as reference). The subsidence values are displayed by a positive vertical deformation measured from the ground surface. The effect of friction on the vertical walls is believed to be minimized by the lubrication effect of the water, not affecting, therefore, the settlement measurements. The interpretation of the data obtained is herein explained for the first cycle of the loose sand (Figure 2). For the saturated soil, both the water level and the soil surface are at the height of 689.0 mm. After the first extraction of water, the water level reduces to a height of 160.0 mm and the soil surface to a height of 688.3 mm, which indicates a total subsidence value of 0.7 mm (the vertical displacement curve moves 0.7 mm downwards). With the first recharging of water, the height of the sand returns to the original height (the vertical displacement curve moves 0.7 mm upwards), thus, the total subsidence for the first cycle is 0 mm. The subsidence values caused per half cycle, including both withdrawing and recharging, and the cumulative subsidence values are presented in Table 5 for the three specimens.

The observations from Figures 2 to 4 indicate that lowering the water table causes soil subsidence while raising the water table, can either reduce land subsidence, that is to say, the sample rebounds, or make subsidence more severe. According to the results, the soil behaviour during water recharging appears to depend on both the initial density of the sample and the number of withdrawal-recharging cycles the material has been subjected to. For loose sand and dense sand, the rebound value due to the first recharging water is nearly equal to the settlement value due to the first withdrawal of water; but for the medium dense sand, the first recharging water tends to increase the subsidence value.

This difference in the initial behaviour of the sand can be explained based on the initial microstructure (or fabric) of the sand specimens. The potential of the soil to deform is known to be dependent not only on soil density but also on the soil fabric (Fonseca et al., 2013a, 2013b). Fonseca et al. (2013a) have quantified the evolution of soil fabric of sands under triaxial loading using, for example, the orientation of the major axis of the grains. For a sand formed of slightly elongated grains as Pingtan sand, dry pluviation (with a significant drop height) tends to produce samples with grains lying with their longer axes in the horizontal plane, whereas tamping tends to create more randomly oriented grains (Nemat-Nasser and Takahashi, 1984). In the present study, the dry pluviation technique (with a drop height of 400 mm) used for the medium dense sample is likely to have induced high anisotropy on the sample caused by the horizontally oriented elongated grains. For the loose sample the almost zero drop high did not allow the grains to reorient while falling and more random distributions are expected. Similarly, for the dense sand, tamping the soil is likely to have altered the depositional orientation of the grains, i.e. the grains rotate slightly in order to fill the available spaces as the material densifies. The deformation of the medium dense sand during recharging shows that the horizontally oriented grains make the soil less prone to rebound following recharging. This observation suggests that more randomly oriented grain can more easily be displaced by the upward movement of the recharging water (unloading), while the horizontally oriented grains create greater resistance to rearrange and move upwards.

Subsequently, the soil deformation caused by the repeated variation of the water table would have contributed to disrupt the initial fabric (and the anisotropy) and the medium sand starts to rebound and have a more similar behaviour to the other specimens. Following these internal rearrangements of the soil structure, the deformation values measured for the different specimens at each stage became more similar (as shown in Table 5). For the second and third withdrawal-recharging cycles, the subsidence caused by water withdrawing is large, while the resilience caused by recharging water is very small, i.e. the subsidence values increase significantly for the three specimens. Along with a large unrecoverable residual deformation (plastic deformation), also significant creep deformation occurs. The creep deformation of the sample at this stage is consistent with the results presented by Zhang et al. (2006).

At the fourth cycle, a new behaviour pattern seems to take place, subsidence due to withdrawing decreases slightly and the rebound deformation due to recharging water increases. Creep deformation is also less obvious at this stage compared with the previous second and third withdrawal-recharging cycles.

4 SAND DEFORMATION UNDER WITHDRAWING AND RECHARGING CONDITIONS

The deformation of the sand caused by the lowering and rising of the water table is investigated by calculating the change in effective stress and strain that the material was subjected to. The variation in effective stress of the soil is calculated according to the additional stress induced by the change in the water level, as illustrated in Figure 5.

Taking the change of water level as Δh, the effective stress acting on the top of sand layer ② (Figure 5) before withdrawal (or after recharging) is $\gamma' \cdot \Delta h$ and the pressure acting on top of sand layer ② after withdrawal (or before recharging) is $\gamma \cdot \Delta h$. The natural or wet unit weight of the sand is usually approximately equal to its saturated weight

$$\gamma \approx \gamma_{\text{sat}} = \gamma_{\text{w}} + \gamma' \tag{1}$$

where γ is the natural (or wet) unit weight of sand; γ_{sat} is the saturated unit weight of sand; γ' is the submerged unit weight of sand; and γ_{w} is the unit weight of water. This formulation assumes that the water table is above the soil surface and the water does not withdraw into the soil.

Therefore, $\gamma \cdot \Delta h$ is approximately equal to $(\gamma'+\gamma_{\text{w}}) \cdot \Delta h$, the additional stress acting on sand soil under water table due to withdrawal shown in Figure 5 can be expressed as follows:

$$\Delta p_2 = \gamma \cdot \Delta h - \gamma' \cdot \Delta h \approx (\gamma_{\text{w}} + \gamma') \cdot \Delta h - \gamma' \cdot \Delta h = \gamma_{\text{w}} \cdot \Delta h \tag{2}$$

where Δp_2 is the additional stress due to the change of water table.

The additional stress acting on sand soil under water table due to recharging can be expressed as follows:

$$\Delta p_2 = \gamma' \cdot \Delta h - \gamma \cdot \Delta h \approx \gamma' \cdot \Delta h - (\gamma_{\text{w}} + \gamma') \cdot \Delta h = -\gamma_{\text{w}} \cdot \Delta h \tag{3}$$

Since the additional stress acting on the sand layer ① varies with a triangular distribution in depth, i.e. from 0 to Δp_2, hence its average variation can be obtained by taking half of the maximum value Δp_2, as follows:

$$\Delta p_1 = \Delta p_2 / 2 \tag{4}$$

where Δp_1 is the average additional stress acting on a sand layer between the initial and final water table levels.

Therefore, the variation of effective stress can be obtained by averaging the additional stress according to the sand thickness above and below the water table, as follows:

$$\begin{aligned} \Delta p &= (\Delta p_1 \cdot \Delta h + \Delta p_2 \cdot h_2)/(\Delta h + h_2) \\ &= \begin{cases} \gamma_{\text{w}} \cdot \Delta h \cdot (\Delta h/2 + h_2)/(\Delta h + h_2) & \text{withdrawal} \\ -\gamma_{\text{w}} \cdot \Delta h \cdot (\Delta h/2 + h_2)/(\Delta h + h_2) & \text{recharging} \end{cases} \end{aligned} \tag{5}$$

where Δp is the effective stress variation acting on the sand due to withdrawal; and h_2 is the depth of water table after withdrawing water.

According to the vertical deformation of the sand at different periods and its original height, the strain can be obtained as follows:

$$\varepsilon = \Delta l / h \tag{6}$$

where Δl is the vertical deformation and h is the original height of the sand.

Based on the measurements of the change in the water level after extracting and recharging water, the effective stress variation was calculated at different stages. Similarly, the strain value (compression strain is positive) was obtained according to the deformation of the sample at the same stages. The plots of strain against

the variation of effective stress are presented in Figures 6, 7 and 8 for the loose, medium dense and dense samples, respectively. For the first withdrawal-recharging cycle, the strain of the loose sample is larger than that of the medium dense and dense samples, as expected. The different compressibility of the three specimens can be inferred from the compression modulus (assuming elastic deformation) values obtained for the loose sand, medium dense sand and dense sand, which were of 3.21MPa, 4.81MPa and 6.93MPa, respectively.

The cyclic withdrawing and recharging of water through the sand contributes to its densification. At the second and third withdrawal-recharging cycles, it can be seen that the strain increases with extracting of water and slightly more in recharging water, which indicates that not only unrecoverable plastic deformation but also hysteretic creep deformation have occurred in the sand. For the fourth withdrawal-recharging cycle and thereafter, both the elastic and the plastic deformations become smaller, and this could be a consequence of the densification of the soil together with the development of a more stable fabric. The strains are also smaller compared to the previous cycles as can be seen from the stress:strain curves of loose and medium dense sands. Judging from the slope of the stress strain curves, as the slope increases, both the compression and resilient moduli (i.e. $\Delta\sigma/\Delta\varepsilon$, when recharging) of loose and medium dense sand become larger. This can be explained based on the densification of the sand and is less clear for the dense sand.

5 STRAIN EVOLUTION WITH THE WITHDRAWAL-RECHARGING CYCLES

Figure 9 shows the evolution of vertical strain with the withdrawal-recharging cycles. It can be observed that the vertical strain increases with the number of cycles. In the same way as the results presented in Figure 2 to 4, generally the strains increase with the water withdrawing (the first half of the cycle) due to the increase of the vertical additional stress and decrease with water recharging (the second half of the cycle). The overall change in strain for a complete cycle depends on the cycle number and the initial density and fabric of the specimen. In the first cycle, the final vertical strain of loose sand and dense sand is nearly zero, which means that the sand behaves as an elastic material. A slightly different trend in the strain evolution can be seen for the medium dense sand, suggesting a more viscoelastic behaviour from the first cycle. Subsequently, with the increase in the number of withdrawal-recharging cycles, the vertical strain increases faster for all samples as the vertical deformation caused by withdrawing is not fully recovered after recharging of water.

6 CONCLUSIONS

Motivated by the lack of studies on land subsidence of sands, this paper presents an experimental investigation on the deformation behaviour of a quartzitic sand exposed to cyclic withdrawal and recharging of groundwater. The observations presented here shed new light on soil characteristics that can potentially affect subsidence and rebound of the material. It has been shown that during the first withdrawal-recharging cycle, the loose and dense samples exhibit elastic behaviour, i.e. the material rebounds by the same amount as it settles during withdrawing. A different behaviour is observed for the medium dense sample and this is attributed to the initial anisotropy of this sample related to the horizontally oriented grains as a result of the sample preparation method. With further withdrawal and recharging, i.e. at the second and third withdrawal-recharging cycles, the vertical deformation of the soil increases significantly. Irreversible plastic deformation and creep deformation

were seen to occur for all samples, in addition, rebound is essentially suppressed. Similar behaviour between the different samples was observed at the third withdrawal-recharging cycle and thereafter suggesting disruption of the initial fabric and the adjustment of the initial density due to soil deformation. At the fourth cycle the overall deformation becomes minor as a consequence of lower deformation on withdrawing and a slight increase in the rebound. Creep deformation is less obvious than at the second and third cycles and the elastic and plastic deformations are smaller. Hypothesis for the observed behaviour at this stage are the densification of the sample together with the development of a more stable fabric. This study revealed patterns of deformation behaviour in sand prepared at different initial density that cannot be explained in view of void ratio alone and further microstructure considerations were discussed. Future work will focus on a microscale investigation on the effect of fabric on the withdrawal and recharging of sands. It is clear from this study that under some circumstances water recharging can be beneficial to reduce land subsidence. It is therefore of utmost importance to establish the soil characteristics for which this measure can be used to control land subsidence.

ACKNOWLEDGMENTS

The investigation was supported by the National Natural Science Foundation of China (No. 50908139), Shanghai University outstanding young teachers scientific research project, China and the State Scholarship Fund of China.

REFERENCES

Allen D.R., Mayuga, M.N., 1969. The Mechanics of Compaction and Rebound, Wilmington Oil Field, Long Beach, California, U.S.A., Land subsidence: proceedings of the Tokyo Symposium,410-423.

Avilés J., Pérez-Rocha L.E., 2010. Regional subsidence of Mexico City and its effects on seismic response. Soil Dynamics and Earthquake Engineering 30, 981-989.

Boukpeti N., Mróz Z., Drescher A., 2004. Modeling rate effects in undrained loading of sands. Canadian Geotechnical Journal 41, 342-350.

Budhu M., 2011. Earth Fissure Formation from the Mechanics of Groundwater Pumping. International Journal of Geomechanics 11,1-11.

Chaussard E., Wdowinski S., Cabral-Cano E., Amelung F., 2014. Land subsidence in central Mexico detected by ALOS InSAR time-series. Remote Sensing of Environment 140, 94-106.

Cui Z.D., Jia Y.J., 2013. Analysis of electron microscope images of soil pore structure for the study of land subsidence in centrifuge model tests of high-rise building groups. Engineering Geology 164, 107-116.

Fodil, A., Aloulou, W., Hicher, P.Y., 1997. Viscoplastic behaviour of soft clay. Géotechnique 47(3), 581-591.

Fonseca J., O'Sullivan C., Coop M.R., Lee, P.D., 2013a. Quantifying the evolution of soil fabric during shearing using scalar parameters. Géotechnique 63(10), 818-829.

Fonseca J., O'Sullivan C., Coop M.R., Lee, P.D., 2013b. Quantifying the evolution of soil fabric during shearing using directional parameters. Géotechnique 63(6), 487-499.

Karim M. R., Gnanendran C. T., Lo S.-C.R., Mark J., 2010. Predicting the long-term performance of a wide embankment on soft soil using an elastic-viscoplastic model. Canadian Geotechnical Journal 47, 244-257.

Kutter, B.L., Sathialingam, N., 1992. Elastic-viscoplastic modelling of the rate-dependent behaviour of clays. Géotechnique 42(3), 427-441.

Lade, P.V., Yamamuro, J.A., Bopp, P.A., 1997. Influence of time effects on instability of granular materials. Computers and Geotechnics 20(3), 179-193.

Luo Z.J., Zeng F., 2011. Finite element numerical simulation of land subsidence and groundwater exploitation based on visco-elastic-plastic Biot's consolidation theory. Journal of Hydrodynamics 23(5), 615-624.

Lv W.H., Miao L.C., Li C.L., 2011. Physical model test of land subsidence caused by groundwater withdrawal. Geo-Frontiers 2011, 1623-1630.

Marsal, R.J., Sáinz O.I., 1956. Breve descripción del hundimiento de la Ciudad de México, paper presented at XX International Geological Congress, Sociedad Geológica Mexicana, Mexico City.

Miao L.C., Zhang Y.J., Wang F., Yuan X.J., 2011. Prediction of land subsidence using a proposed consolidation-seepage-creep coupling model. Geo-Frontiers 2011,1631-1640.

Ministry of land and resources of the People's Republic of China, Ministry of water resources of the People's Republic of China, 2012. The ground subsidence control planning in China (2011-2020).

Nemat-Nasser S., Takahashi K., 1984. Liquefaction and fabric of sand. Journal of Geotechnical engineering 110(9), 1291-1306.

Ortiz, Z. D., Ortega G. A., 2010. Evolution of long-term land subsidence near Mexico City: Review, field investigations, and predictive simulations. Water Resources Research 46,W01513.

Pacheco-Martínez J., Hernandez-Marín M., Burbey T.J., González-Cervantes N., Ortíz-Lozano J.A., Zermeño-De-Leon M.E., Solís-Pinto A., 2013. Land subsidence and ground failure associated to groundwater exploitation in the Aguascalientes Valley, México. Engineering Geology 164,172-186.

Pan M., Li T. F., 2012. Geologic Hazards (2nd Edition). Peking University press, Beijing. (in Chinese).

Phien-wej N., Giao P.H., Nutalaya P., 2006. Land subsidence in Bangkok, Thailand. Engineering Geology 82,187-201.

Sato H. P., Abe K., Ootaki, O., 2003. GPS-measured land subsidence in Ojiya City, Niigata Prefecture, Japan. Engineering Geology 67,379-390.

Shi L.X., Bao M.F., 1984. Case history No.9.2: Shanghai, China. In guidebook to studies of land subsidence due to ground-water withdrawal, Edited by: Poland, J.F. 155-160. Paris: UNESCO.

Shi X.Q., Wu J.C., Ye S.J., Zhang Y., Xue Y.Q., Wei Z.X., Li Q.F., Yu J., 2008. Regional land subsidence simulation in Su-Xi-Chang area and Shanghai City, China. Engineering Geology 100, 27-42.

Teatini P., Ferronato M., Gambolati G., Bertoni W., Gonella M., 2005. A century of land subsidence in Ravenna, Italy. Environmental Geology 47(6),831-846.

Tomas R., Herrera G., Lopez-Sanchez J.M., Vicente F., Cuenca A., Mallorquí J.J., 2010. Study of the land subsidence in Orihuela City (SE Spain) using PSI data: Distribution, evolution and correlation with conditioning and triggering factors. Engineering Geology 115,105-121.

Tung H., Hu J.C., 2012. Assessments of serious anthropogenic land subsidence in Yunlin County of central Taiwan from 1996 to 1999 by Persistent Scatterers InSAR. Tectonophysics 578,126-135.

Wang G.Y., You G., Shi B., Yu J., Tuck M., 2009. Long-term land subsidence and strata compression in Changzhou, China. Engineering Geology 104, 109-118.

Wu J.C., Shi X.Q., Ye S.J., Xue Y.Q., Zhang Y., Wei Z.X., Fang Z., 2010. Numerical Simulation of viscoelastoplastic land subsidence due to groundwater overdrafting in Shanghai, China. Journal of hydrologic engineering 15(3), 223-236.

Ye S.J., Xue Y.Q., Zhang Y., Li Q.F., Wang H.M., 2005. Study on the deformation characteristics of soil layers in regional land subsidence model of Shanghai. Chinese Journal of Geotechnical Engineering 27(2), 140-147. (in Chinese)

Yin J. H., Zhu J.G., 1999. Elastic viscoplastic consolidation modelling and interpretation of pore-water pressure responses in clay underneath Tarsiut Island. Canadian Geotechnical Journal 36, 708-717.

Yin J.H., Zhu J.G., Graham J., 2002. A new elastic viscoplastic model for time-dependent behaviour of normally and overconsolidated clays: theory and verification. Canadian Geotechnical Journal 39, 157-173.

Zhang Y., Xue Y.Q., Wu J.C., Li Q.F., 2006. Characteristics and parameters of sand strata deformation due to groundwater pumping in Shanghai. Journal of Hydraulic Engineering 37(5),560-566. (in Chinese)

Zhang Y., Xue Y.Q., Wu J.C., Wang H.M., He J.J., 2012. Mechanical modeling of aquifer sands under long-term groundwater withdrawal. Engineering Geology 125, 74-80.

Zheng W.L., Si G.P., Zheng X.H., 2005. Groundwater calamity in environmental geotechnics in urban areas. The Chinese Journal of Geological Hazard and Control 16(3), 67-70. (in Chinese)

Table 1 Particle size distribution for the Pingtan sand

Particle Diameter (mm)	<0.25	0.25-0.45	0.45-0.65	>0.65
Content (%)	6	51±5	40±5	3

Table 2 Particle size distribution characteristic parameters

d_{50} (mm)	C_u	C_c
0.340	1.542	1.104

Table 3 Physical indexes

ρ_{dmax} (g/cm^3)	ρ_{dmin} (g/cm^3)	G_s (g/cm^3)	e_{max}	e_{min}
1.74	1.43	2.643	0.848	0.519

Table 4 Preparation techniques and physical parameters for each sample

Specimen	Sample preparation technique	Void ratio	Relative density	Density (kg/m^3)
Loose sand	Dry pluviation with a fall height of nearly 0 mm.	0.775	0.222	1489
Medium dense sand	Dry pluviation with a fall height of 400 mm.	0.731	0.356	1527
Dense sand	Combination of dry pluviation (400 mm fall height) with tamping using a hammer of 2.5 kg weight at the sample heights of 250 mm, 500mm and 700 mm.	0.577	0.824	1676

Table 5 Subsidence values due to withdrawal and recharging

	Subsidence value per half cycle (mm)			Cumulative subsidence value (mm)		
	Loose sand	Medium dense sand	Dense sand	Loose sand	Medium dense sand	Dense sand
First withdrawal	0.7	0.4	0.3	0.7	0.4	0.3
First recharging	-0.7	0.7	-0.3	0	1.1	0
Second withdrawal	1.3	0.6	0.7	1.3	1.7	0.7
Second recharging	-0.1	0.8	0.5	1.2	2.5	1.2
Third withdrawal	1.1	0.5	1.2	2.3	3.0	2.4
Third recharging	0.2	-0.3	-0.3	2.5	2.7	2.1
Fourth withdrawal	0.8	0.8	1.1	3.3	3.5	3.2
Fourth recharging	-0.6	-0.4	0	2.7	3.1	3.2
Fifth withdrawal	0.8	0.5	0.7	3.5	3.6	3.9
Fifth recharging	-0.5	-0.5	-	3.0	3.1	-
Sixth withdrawal	1.0	1.0	-	4.0	4.1	-

Note: Negative value means rebound deformation.

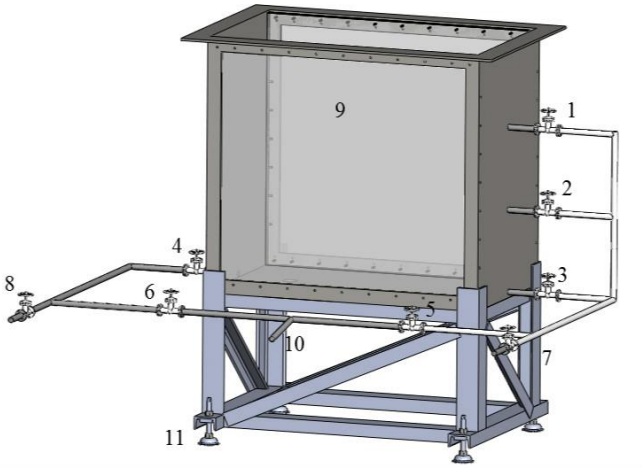

(a) Front and right side views

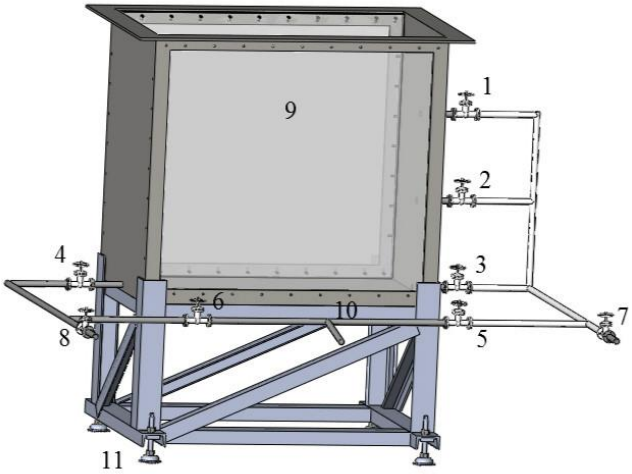

(b) Front view and left side views

1,2,3,4 Inlet/Outlet valve 5,6 Inlet valve

7,8 Outlet valve 9 Glass panel

10 Inlet pipe 11 Support frame

Figure 1 Lateral and front views of the model box and pipes

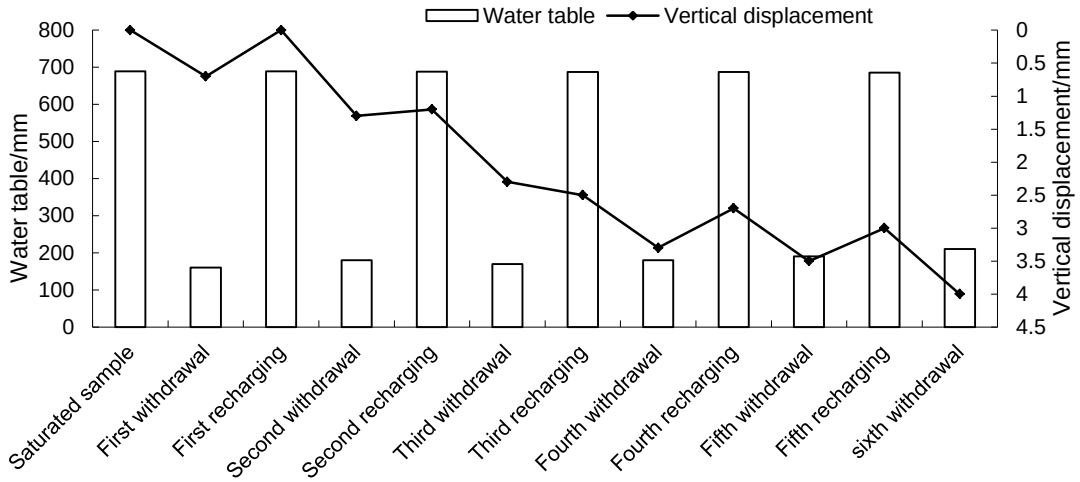

Figure 2 Variation of water table and vertical deformation for the loose sand

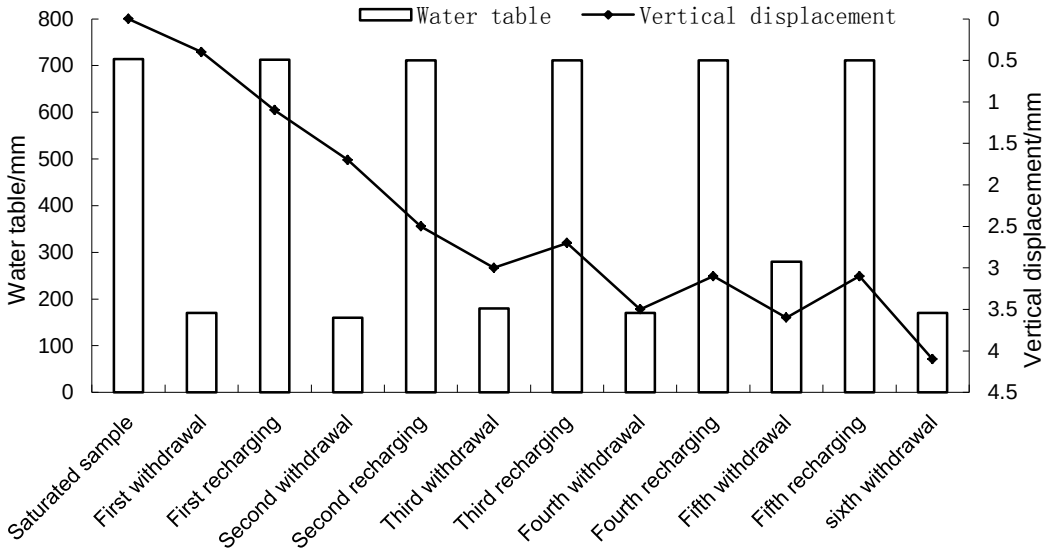

Figure 3 Variation of water table and vertical deformation for the medium dense sand

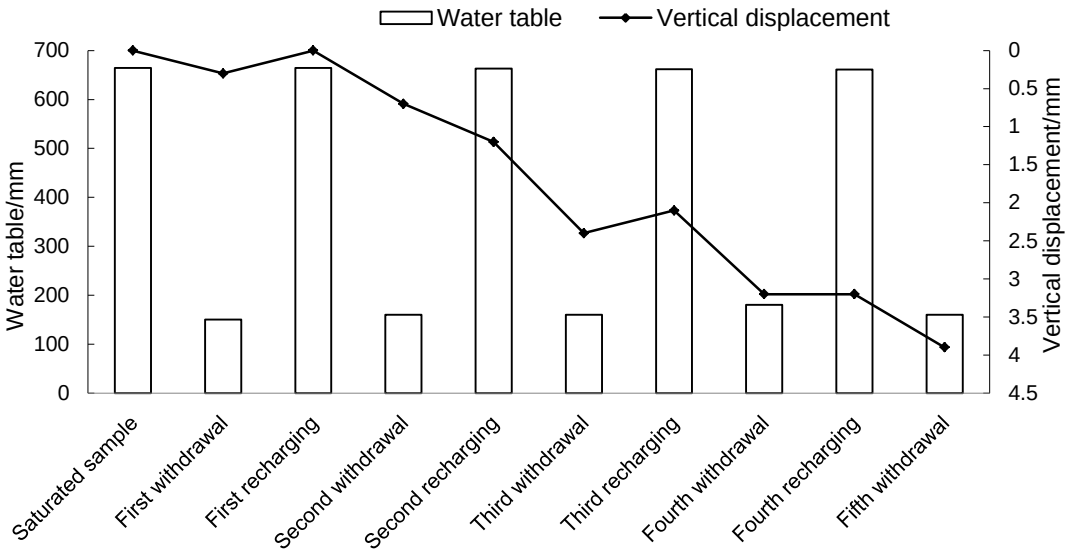

Figure 4 Variation of water table and vertical deformation for the dense sand

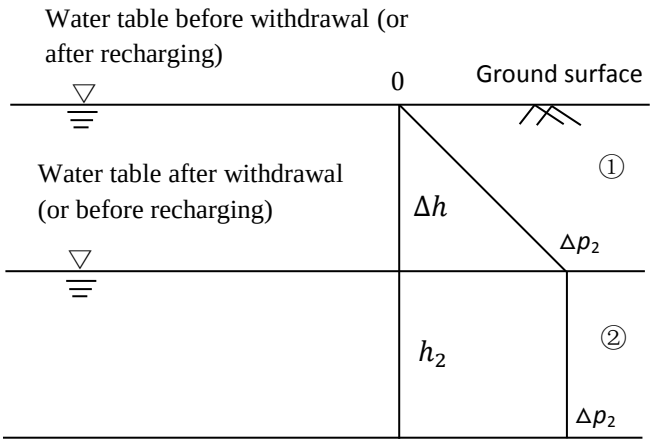

Figure 5 Sketch of the additional stress distribution

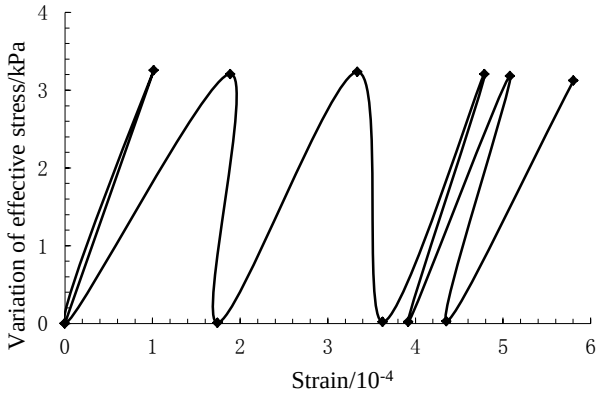

Figure 6 Stress:strain plot for the loose sand

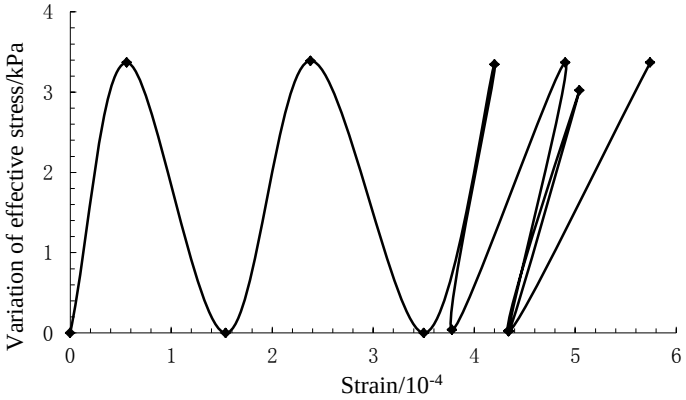

Figure 7 Stress:strain plot for the medium dense sand

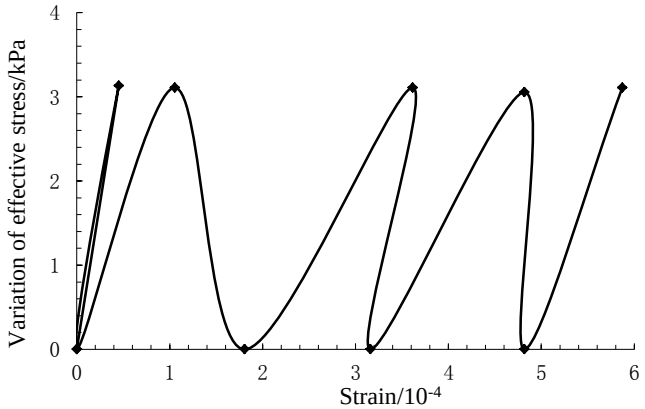

Figure 8 Stress:strain plot for the dense sand

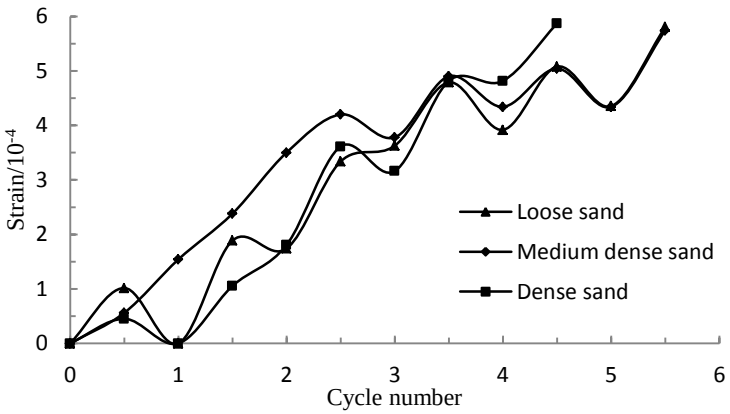

Figure 9 Strain evolution with the number of cycles